Study of the decays $B \to D_{s1}(2536)^+ \bar{D}^{(*)}$

T. Aushev,[15] I. Adachi,[10] K. Arinstein,[1,36] V. Aulchenko,[1,36] A. M. Bakich,[43] V. Balagura,[15] V. Bhardwaj,[38] M. Bischofberger,[28] A. Bondar,[1,36] A. Bozek,[32] M. Bračko,[24,16] T. E. Browder,[9] M.-C. Chang,[4] A. Chen,[29] P. Chen,[31] B. G. Cheon,[8] R. Chistov,[15] I.-S. Cho,[54] K. Cho,[19] K.-S. Choi,[54] Y. Choi,[42] J. Dalseno,[25,45] M. Danilov,[15] A. Drutskoy,[3] S. Eidelman,[1,36] D. Epifanov,[1,36] V. Gaur,[44] N. Gabyshev,[1,36] A. Garmash,[1,36] B. Golob,[23,16] H. Ha,[20] K. Hayasaka,[27] H. Hayashii,[28] Y. Horii,[48] Y. Hoshi,[47] W.-S. Hou,[31] H. J. Hyun,[21] T. Iijima,[27] K. Inami,[27] A. Ishikawa,[39] R. Itoh,[10] M. Iwabuchi,[54] Y. Iwasaki,[10] T. Iwashita,[28] T. Julius,[26] J. H. Kang,[54] T. Kawasaki,[34] H. J. Kim,[21] H. O. Kim,[21] J. H. Kim,[19] M. J. Kim,[21] Y. J. Kim,[7] K. Kinoshita,[3] B. R. Ko,[20] P. Kodyš,[2] P. Križan,[23,16] T. Kuhr,[18] T. Kumita,[50] A. Kuzmin,[1,36] Y.-J. Kwon,[54] S.-H. Kyeong,[54] J. S. Lange,[5] S.-H. Lee,[20] J. Li,[9] C. Liu,[40] Y. Liu,[31] D. Liventsev,[15] R. Louvot,[22] A. Matyja,[32] S. McOnie,[43] K. Miyabayashi,[28] H. Miyata,[34] Y. Miyazaki,[27] R. Mizuk,[15] G. B. Mohanty,[44] M. Nakao,[10] H. Nakazawa,[29] Z. Natkaniec,[32] S. Neubauer,[18] S. Nishida,[10] O. Nitoh,[51] S. Ogawa,[46] T. Ohshima,[27] S. L. Olsen,[41,9] W. Ostrowicz,[32] P. Pakhlov,[15] G. Pakhlova,[15] H. K. Park,[21] R. Pestotnik,[16] M. Petrič,[16] L. E. Piilonen,[52] A. Poluektov,[1,36] K. Prothmann,[25,45] M. Röhrken,[18] S. Ryu,[41] H. Sahoo,[9] K. Sakai,[10] Y. Sakai,[10] O. Schneider,[22] C. Schwanda,[13] K. Senyo,[27] O. Seon,[27] M. E. Sevior,[26] M. Shapkin,[14] V. Shebalin,[1,36] C. P. Shen,[9] J.-G. Shiu,[31] B. Shwartz,[1,36] F. Simon,[25,45] J. B. Singh,[38] P. Smerkol,[16] Y.-S. Sohn,[54] A. Sokolov,[14] E. Solovieva,[15] S. Stanič,[35] M. Starič,[16] M. Sumihama,[55,6] T. Sumiyoshi,[50] S. Tanaka,[10] Y. Teramoto,[37] I. Tikhomirov,[15] K. Trabelsi,[10] M. Uchida,[55,49] T. Uglov,[15] S. Uno,[10] Y. Usov,[1,36] S. E. Vahsen,[9] G. Varner,[9] K. Vervink,[22] A. Vinokurova,[1,36] A. Vossen,[11] C. H. Wang,[30] M.-Z. Wang,[31] P. Wang,[12] Y. Watanabe,[17] K. M. Williams,[52] B. D. Yabsley,[43] Y. Yamashita,[33] Y. Yusa,[52] Z. P. Zhang,[40] V. Zhilich,[1,36] P. Zhou,[53] V. Zhulanov,[1,36] A. Zupanc,[18] and O. Zyukova[1,36]

(The Belle Collaboration)

[1] *Budker Institute of Nuclear Physics, Novosibirsk*
[2] *Faculty of Mathematics and Physics, Charles University, Prague*
[3] *University of Cincinnati, Cincinnati, Ohio 45221*
[4] *Department of Physics, Fu Jen Catholic University, Taipei*
[5] *Justus-Liebig-Universität Gießen, Gießen*
[6] *Gifu University, Gifu*
[7] *The Graduate University for Advanced Studies, Hayama*
[8] *Hanyang University, Seoul*
[9] *University of Hawaii, Honolulu, Hawaii 96822*
[10] *High Energy Accelerator Research Organization (KEK), Tsukuba*
[11] *University of Illinois at Urbana-Champaign, Urbana, Illinois 61801*
[12] *Institute of High Energy Physics, Chinese Academy of Sciences, Beijing*
[13] *Institute of High Energy Physics, Vienna*
[14] *Institute of High Energy Physics, Protvino*
[15] *Institute for Theoretical and Experimental Physics, Moscow*
[16] *J. Stefan Institute, Ljubljana*
[17] *Kanagawa University, Yokohama*
[18] *Institut für Experimentelle Kernphysik, Karlsruher Institut für Technologie, Karlsruhe*
[19] *Korea Institute of Science and Technology Information, Daejeon*
[20] *Korea University, Seoul*
[21] *Kyungpook National University, Taegu*
[22] *École Polytechnique Fédérale de Lausanne (EPFL), Lausanne*
[23] *Faculty of Mathematics and Physics, University of Ljubljana, Ljubljana*
[24] *University of Maribor, Maribor*
[25] *Max-Planck-Institut für Physik, München*
[26] *University of Melbourne, School of Physics, Victoria 3010*
[27] *Nagoya University, Nagoya*
[28] *Nara Women's University, Nara*
[29] *National Central University, Chung-li*
[30] *National United University, Miao Li*
[31] *Department of Physics, National Taiwan University, Taipei*
[32] *H. Niewodniczanski Institute of Nuclear Physics, Krakow*
[33] *Nippon Dental University, Niigata*

[34] Niigata University, Niigata
[35] University of Nova Gorica, Nova Gorica
[36] Novosibirsk State University, Novosibirsk
[37] Osaka City University, Osaka
[38] Panjab University, Chandigarh
[39] Saga University, Saga
[40] University of Science and Technology of China, Hefei
[41] Seoul National University, Seoul
[42] Sungkyunkwan University, Suwon
[43] School of Physics, University of Sydney, NSW 2006
[44] Tata Institute of Fundamental Research, Mumbai
[45] Excellence Cluster Universe, Technische Universität München, Garching
[46] Toho University, Funabashi
[47] Tohoku Gakuin University, Tagajo
[48] Tohoku University, Sendai
[49] Tokyo Institute of Technology, Tokyo
[50] Tokyo Metropolitan University, Tokyo
[51] Tokyo University of Agriculture and Technology, Tokyo
[52] CNP, Virginia Polytechnic Institute and State University, Blacksburg, Virginia 24061
[53] Wayne State University, Detroit, Michigan 48202
[54] Yonsei University, Seoul
[55] Research Center for Nuclear Physics, Osaka

We report a study of the decays $B \to D_{s1}(2536)^+ \bar{D}^{(*)}$, where $\bar{D}^{(*)}$ is $\bar{D}^0$, D^- or D^{*-}, using a sample of 657×10^6 $B\bar{B}$ pairs collected at the $\Upsilon(4S)$ resonance with the Belle detector at the KEKB asymmetric-energy e^+e^- collider. The branching fractions of the decays $B^+ \to D_{s1}(2536)^+ \bar{D}^0$, $B^0 \to D_{s1}(2536)^+ D^-$ and $B^0 \to D_{s1}(2536)^+ D^{*-}$ multiplied by that of $D_{s1}(2536)^+ \to (D^{*0}K^+ + D^{*+}K^0)$ are found to be $(3.97 \pm 0.85 \pm 0.56) \times 10^{-4}$, $(2.75 \pm 0.62 \pm 0.36) \times 10^{-4}$ and $(5.01 \pm 1.21 \pm 0.70) \times 10^{-4}$, respectively. The ratio $\mathcal{B}(D_{s1} \to D^{*0}K^+)/\mathcal{B}(D_{s1} \to D^{*+}K^0)$ is measured to be $0.88 \pm 0.24 \pm 0.08$.

PACS numbers: 13.25.Hw, 14.40.Lb, 14.40.Nd

The $D_{s1}(2536)^+$ is a narrow P-wave resonance for which the $J^P = 1^+$ assignment is strongly favored [1]. Although the $D_{s1}(2536)^+$ was first observed in 1989 [2], its properties are still not well measured. In this analysis we study the production of $D_{s1}(2536)^+$ in doubly charmed B meson decays, $B \to D_{s1}(2536)^+ \bar{D}^{(*)}$, where $\bar{D}^{(*)}$ is either a $\bar{D}^0$, D^- or D^{*-} [3]. The branching fraction measurements of the decays $B \to D_{s1}(2536)^+ \bar{D}^{(*)}$ together with those of $B \to \bar{D}^{(*)} D^{(*)}_{s(J)}$ decays provide important information to check the molecular hypothesis for the $D^*_{s0}(2317)$ and $D_{s1}(2460)$ particles [4, 5]. First observations of the $B \to D_{s1}(2536)^+ \bar{D}^{(*)}$ decay modes have been reported by BaBar [6, 7]. An upper limit on the decay $B^0 \to D_{s1}(2536)^+ D^{*-}$ was also obtained by Belle [8], which is consistent with the BaBar measurement.

This analysis is based on $605\,\mathrm{fb}^{-1}$ of data collected at the $\Upsilon(4S)$ resonance with the Belle detector [9] at the KEKB asymmetric-energy e^+e^- collider [10], which corresponds to 657×10^6 $B\bar{B}$ pairs. The Belle detector is a general-purpose spectrometer with a 1.5 T magnetic field provided by a superconducting solenoid. A silicon vertex detector and a 50-layer central drift chamber are used to measure the momenta of charged particles. Photons are detected in an electromagnetic calorimeter consisting of CsI(Tl) crystals. Particle identification likelihoods $\mathcal{L}_K$ and $\mathcal{L}_\pi$ are derived from information provided by an array of time-of-flight counters, an array of silica aerogel Cherenkov threshold counters and dE/dx measurements in the central drift chamber. Two inner detector configurations were used. A 2.0 cm radius beampipe and a 3-layer silicon vertex detector were used for the first sample of 152×10^6 $B\bar{B}$ pairs, while a 1.5 cm radius beampipe, a 4-layer silicon detector and a small-cell inner drift chamber were used to record the remaining 505×10^6 $B\bar{B}$ pairs.

All charged tracks are required to have a distance of closest approach to the interaction point (IP) in the plane perpendicular to the beam axis smaller than 2 cm and smaller than 5 cm along the beam axis. Charged kaon and pion candidates are required to be positively identified. The K^0_S candidates are reconstructed in the $\pi^+\pi^-$ mode with the requirement $|M_{\pi\pi} - m_{K^0_S}| < 15$ MeV/c^2 (3σ), where $m_{K^0_S}$ is the K^0_S mass [1]. Requirements on the K^0_S vertex displacement from the IP and on the difference between the vertex and K^0_S flight directions are applied. No pion identification is required for the pions from K^0_S candidates. A mass- and vertex-constrained fit is applied to improve the four-momentum measurements of K^0_S candidates. Photons are reconstructed in the electromagnetic calorimeter from showers that are not associated with charged tracks with energies larger than 50 MeV. Combinations of two photons are considered to be π^0 candidates if their invariant mass lies within ± 15 MeV/c^2 (3σ) of the π^0 mass [1]. To improve their

momentum resolution, all π^0 candidates are fitted with a π^0 mass constraint. Continuum $e^+e^- \to q\bar{q}$ backgrounds ($q = u, d, s, c$) are suppressed by requiring the ratio of the second and zeroth Fox-Wolfram moments [11] to be smaller than 0.3.

Candidate D^0's are reconstructed using five decay modes: $K^-\pi^+$, $K^-\pi^+\pi^+\pi^-$, $K^-\pi^+\pi^0$, $K^0_S\pi^+\pi^-$ and K^+K^-. The D^- is reconstructed via its decay into $K^+\pi^-\pi^-$. The selected combinations are constrained to a common vertex and the $\chi^2/n.d.f.$ of the vertex fit is required to be smaller than 25. A ± 15 MeV/c^2 (2σ) mass window around the D^0 mass [1] is used to select D^0 candidates for the $D^0 \to K^-\pi^+\pi^0$ mode and ± 12 MeV/c^2 ($\approx 3\sigma$) for the other D decay modes. To reduce the large combinatorial background in the $D^0 \to K^-\pi^+\pi^0$ decay mode, the energy of each photon from π^0 is required to be greater than 100 MeV. For the $\bar{D}^0$'s coming directly from B decay, only the cleanest modes, $K^+\pi^-$, $K^0_S\pi^+\pi^-$ and K^+K^-, are used. A mass- and vertex-constrained fit is applied for all D candidates. The D^{*+} is reconstructed via its decay to $D^0\pi^+_{\rm slow}$. To improve the $\pi^+_{\rm slow}$ momentum resolution, and thus the D^{*+} mass resolution, the $\pi^+_{\rm slow}$ is constrained to the D^{*+} decay vertex, which is obtained by fitting the D^0 to the IP profile. The D^{*+} candidates with invariant mass within ± 2 MeV/c^2 (4σ) of the D^{*+} [1] mass are selected. The D^{*0} is reconstructed using the $D^0\pi^0$ and $D^0\gamma$ decay modes with invariant mass windows of ± 3 MeV/c^2 and ± 12 MeV/c^2 (2σ), respectively. In both cases a mass-constrained fit is performed for D^{*0} candidates.

The $D_{s1}(2536)^+$ meson is reconstructed in its dominant decay modes: $D^{*0}K^+$ and $D^{*+}K^0_S$. The invariant mass of the $D_{s1}(2536)^+$ candidates is required to be less than 2.58 GeV/c^2. Combinations of $D_{s1}(2536)^+$ and a second charm $\bar{D}^{(*)}$ meson ($\bar{D}^{(*)} = \bar{D}^0$, D^-, D^{*-}) with opposite charm flavor are considered as B meson candidates. B candidates are identified using the energy difference $\Delta E = E_B - E_{\rm beam}$ and beam-energy constrained mass $M_{\rm bc} = \sqrt{E^2_{\rm beam} - p^{*2}_B}$, where E_B and p^*_B are the B candidate energy and momentum in the center-of-mass system, respectively. We require $|\Delta E| < 0.1$ GeV and $M_{\rm bc} > 5.22$ GeV/c^2 to preselect B candidates. After these selections the average candidate multiplicity per event is 1.6. A single candidate per event is chosen based on the smallest χ^2 of the $D^{(*)}$ candidates mass deviations from their nominal values. The ΔE versus $M_{\rm bc}$ scatter plot for the candidates with $D_{s1}(2536)^+$ mass within ± 5 MeV/c^2 (3σ) of the nominal value [1] is presented in Fig. 1 left, for the sum of all studied decay modes. A signal box is defined as $|\Delta E| < 0.02$ GeV and $M_{\rm bc} > 5.27$ GeV/c^2 (region "a"). The $\Delta E - M_{\rm bc}$ two-dimensional sideband is defined as $M_{\rm bc} < 5.26$ GeV/c^2 or $|\Delta E| > 0.03$ GeV (region "b"). The $M_{\rm bc}$ (ΔE) projection is shown for the events with $|\Delta E| < 0.02$ GeV ($M_{\rm bc} > 5.27$ GeV/c^2) in Fig. 1 center (right).

A two-dimensional binned likelihood fit is performed to the $\Delta E - M_{\rm bc}$ distribution and yields 151 ± 15 signal events. The signal yield obtained from the $\Delta E - M_{\rm bc}$ fit contains a contribution from non-resonant $B \to D^* K \bar{D}^{(*)}$ decays that have the same final state particles as the signal. Therefore to extract the yields of each decay mode, we perform an additional binned likelihood fit to the $D_{s1}(2536)^+$ mass distributions for the events in the $\Delta E - M_{\rm bc}$ signal box (Fig. 2). In total, there are nine reconstructed decay modes corresponding to three B meson decay modes, $B^+ \to D_{s1}(2536)^+\bar{D}^0$, $B^0 \to D_{s1}(2536)^+D^-$ and $B^0 \to D_{s1}(2536)^+D^{*-}$, and three $D_{s1}(2536)$ meson decay modes, $D_{s1}(2536)^+ \to D^{*0}(D^0\gamma)K^+$, $D^{*0}(D^0\pi^0)K^+$ and $D^{*+}(D^0\pi^+)K^0_S$. The latter are related by the known branching ratios $R' = \mathcal{B}(D^{*0} \to D^0\pi^0)/\mathcal{B}(D^{*0} \to D^0\gamma) = 1.74 \pm 0.13$ and $R'' = \mathcal{B}(D_{s1}(2536)^+ \to D^{*0}K^+)/\mathcal{B}(D_{s1}(2536)^+ \to D^{*+}K^0) = 1.36 \pm 0.20$ [1]. The shapes of the signal distributions are taken to be a non-relativistic Breit-Wigner functions convolved with the $D_{s1}(2536)^+$ mass resolution function. The Breit-Wigner mass and width of $D_{s1}(2536)^+$ are floating parameters common to all modes. The $D_{s1}(2536)^+$ mass resolution is parametrized by a double Gaussian; the resolution parameters and reconstruction efficiencies are obtained from Monte Carlo (MC) simulation and are summarized in Table I. The shape of the background is parametrized with an ARGUS function [12] and fixed from a fit to events in the $\Delta E - M_{\rm bc}$ sideband. This background function includes both the non-resonant component and the combinatorial background since their shapes are expected to be similar. All nine distributions are fitted simultaneously. The ratios of signal yields in different $D_{s1}(2536)^+$ decay modes are fixed using their relative branching fractions, R' and R'', and MC reconstruction efficiencies. The number of signal events for each of the B decay modes is floated in the fit as a sum of the signal events in all $D_{s1}(2536)^+$ decay modes; the background normalization is free for each distribution. The results of the fit are presented in Table II. The significance is calculated from $\mathcal{S} = \sqrt{-2\ln(\mathcal{L}_0/\mathcal{L}_{\rm max})}$, where $\mathcal{L}_0$ and $\mathcal{L}_{\rm max}$ are the maximized likelihoods with the signal yield fixed at zero and left free, respectively. The $D_{s1}(2536)^+$ mass is found to be 2534.1 ± 0.6 MeV/c^2 and the width is $\Gamma = 0.75 \pm 0.23$ MeV/c^2, consistent with the current world-average values in [1]. To provide a

TABLE I: The products of the total efficiencies and intermediate branching fractions, $\epsilon\mathcal{B}$, and the $D_{s1}(2536)^+$ mass resolution parameters, where $\sigma_{\rm main}$ ($\sigma_{\rm tail}$) is the width of the narrow (wide) Gaussian component, and $f_{\rm tail}$ is the fraction of the wide component.

D_{s1} mode:	$D^{*0}(D^0\gamma)K^+$	$D^{*0}(D^0\pi^0)K^+$	$D^{*+}K_S$
$\epsilon\mathcal{B}(D_{s1}\bar{D}^0)$, 10^{-4}	1.45	1.18	0.74
$\epsilon\mathcal{B}(D_{s1}D^-)$, 10^{-4}	1.97	1.62	1.00
$\epsilon\mathcal{B}(D_{s1}D^{*-})$, 10^{-4}	0.93	0.75	0.32
$\sigma_{\rm main}$, MeV/c^2	1.02	1.01	0.95
$\sigma_{\rm tail}$, MeV/c^2	5.44	3.61	2.43
$f_{\rm tail}$	0.23	0.34	0.15

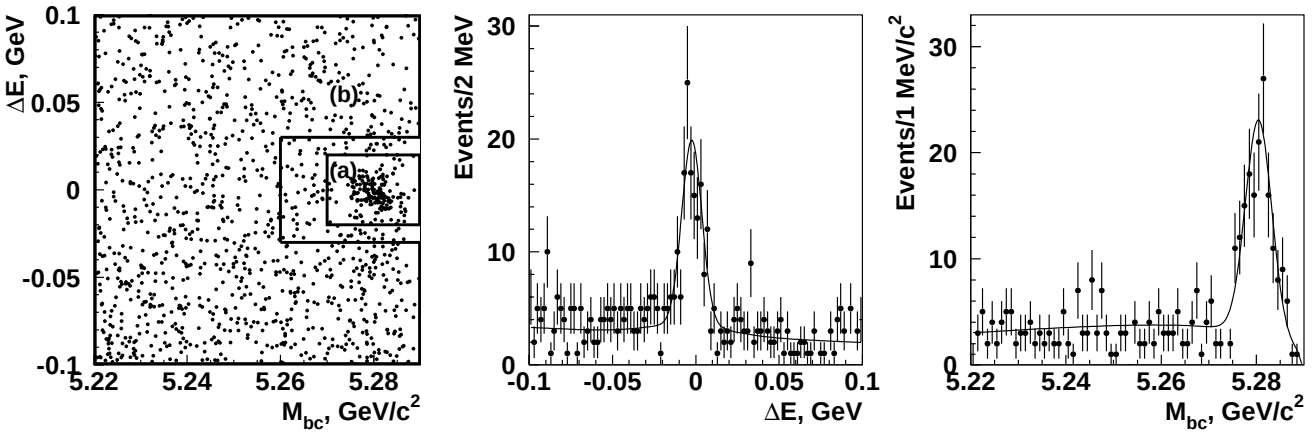

FIG. 1: The scatter plot of ΔE vs $M_{\rm bc}$ (left), where (a) is the signal region and (b) is the sideband, and projections on ΔE for events with $M_{\rm bc} > 5.27$ GeV/c^2 (center) and $M_{\rm bc}$ for events with $|\Delta E| < 0.02$ GeV (right). The $M_{\rm bc}$ distribution is parametrized with a single Gaussian for the signal and an ARGUS function [12] for the background. The ΔE is parametrized with a double Gaussian and a linear polynomial for the signal and background, respectively. The results of the fits are shown by the superimposed curves.

measurement of the $D_{s1}(2536)^+$ branching-fractions ratio another fit is performed with a floating R'' parameter. From the fit we obtain $R'' = 0.88 \pm 0.24$, consistent with other measurements [1].

TABLE II: Summary of the fit results: event yields, branching fractions, and statistical significances.

B decay mode	N	$\mathcal{B}$, 10^{-4}	$\mathcal{S}$
$D_{s1}(2536)^+(D^*K)\bar{D}^0$	42.5 ± 8.7	3.97 ± 0.85	7.0σ
$D_{s1}(2536)^+(D^*K)D^-$	40.2 ± 8.6	2.75 ± 0.62	6.9σ
$D_{s1}(2536)^+(D^*K)D^{*-}$	33.3 ± 7.6	5.01 ± 1.21	6.3σ

The main systematics for the branching fraction measurements is from the tracking efficiency. A 1% systematic error is assigned for each track and an additional 3% error for each low momentum track, which are summed linearly. For the kaon identification a 1% systematic uncertainty is assigned for each kaon track. The contributions of the systematic uncertainties of the K^0_S and γ/π^0 reconstruction efficiencies to the overall systematics are estimated to be 1% and 3%, respectively. The width of the narrow Gaussian component of the signal mass resolution is increased by 20% to obtain the systematics due to the poorer resolution in data compared to MC simulation. To obtain the systematics due to the imperfect background shape description, we vary the shape of the function describing the background: the parameters of the ARGUS function are varied within their errors; we also fix the shape to the one obtained from the generic MC simulation, or use a square root function instead of the ARGUS function. The largest difference in the results is treated as the systematic uncertainty in the background shape description. A possible contribution from inclusive $B \to D_{s1}(2536)^+X$ and $q\bar{q} \to D_{s1}(2536)^+X$ production is checked by examining the $D_{s1}(2536)^+$ mass distribution in a $B\bar{B}$ MC simulation from which the signal has been removed, and in data in the $\Delta E - M_{\rm bc}$ sideband; no signal is found in both cases, so an upper limit on the yield is used as the systematic uncertainty due to the peaking background. Another systematic uncertainty is from the errors in the fractions R' and R'' of the D^{*0} and $D_{s1}(2536)^+$ subdecay modes, respectively. These ratios are varied in the fit within their errors, and the difference in the fit results are assigned as a systematic uncertainty. All the individual systematic errors, shown in Table III, are summed in quadrature. Since the total systematic uncertainty is nearly symmetric, the maximum of the positive and negative errors is taken as the final systematic uncertainty. The errors in the results are dominated by statistical uncertainties.

TABLE III: Relative systematic errors for the branching fractions and the ratio of the branching fractions, $\mathcal{B}(D_{s1} \to D^{*0}K^+)/\mathcal{B}(D_{s1} \to D^{*+}K^0)$, in %.

Source	$\mathcal{B}(D_{s1}\bar{D}^0)$	$\mathcal{B}(D_{s1}D^-)$	$\mathcal{B}(D_{s1}D^{*-})$	R''
Tracking	± 9	± 9	± 9	± 3
Particle ID	± 3	± 3	± 3	± 1
γ/π^0	± 3	± 3	± 3	± 3
K_S	± 1	± 1	± 1	± 1
MC resolution	± 3	± 3	± 3	± 6
BG shape	± 4	± 4	± 4	± 3
Peaking background	$^{+0}_{-3}$	$^{+0}_{-3}$	$^{+0}_{-3}$	± 3
$\mathcal{B}(D^{(*)})$	± 7	± 5	± 7	± 2
R'	± 1	± 1	± 1	± 1
R''	± 1	± 1	± 1	–
$N(B\bar{B})$	± 1.5	± 1.5	± 1.5	–
Total	± 14	± 13	± 14	± 9

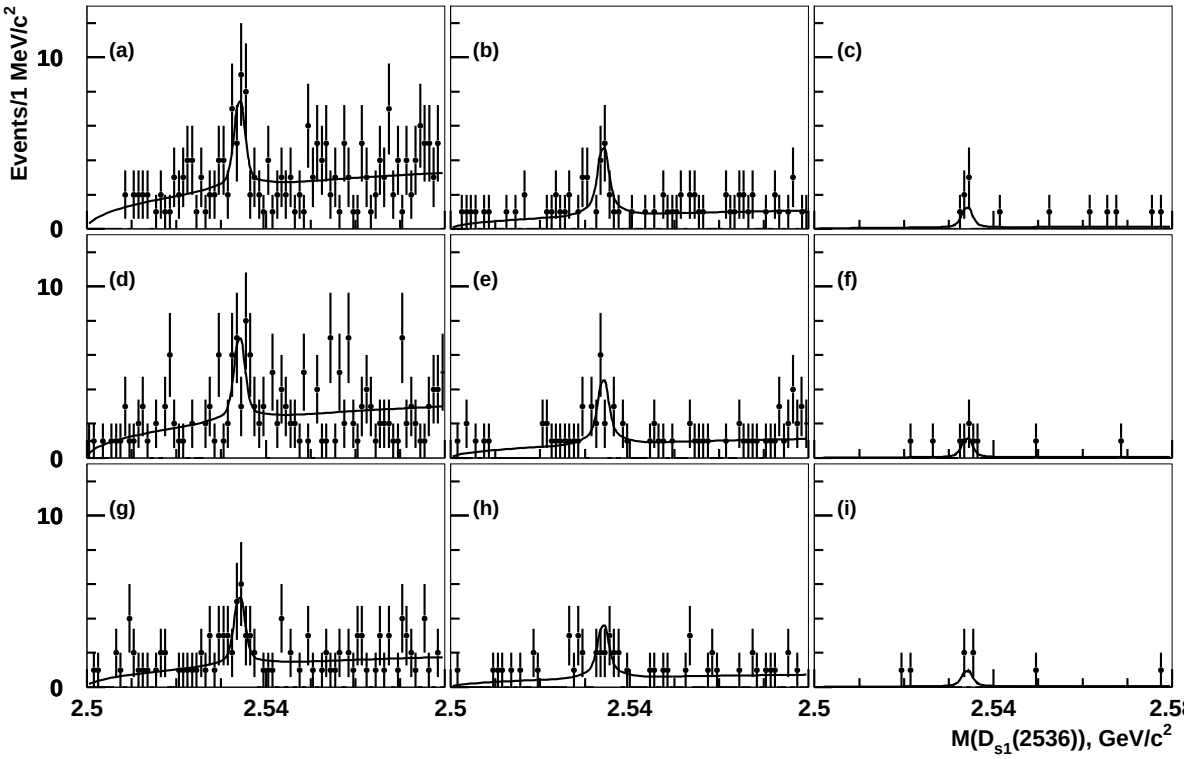

FIG. 2: $D_{s1}(2536)^+$ mass distributions for: a), b), c) $B^+ \to D_{s1}(2536)^+\bar{D}^0$; d), e), f) $B^0 \to D_{s1}(2536)^+D^-$ and g), h), i) $B^0 \to D_{s1}(2536)^+D^{*-}$ final states, followed by $D_{s1}(2536)^+$ decays to a), d), g) $D^{*0}(D^0\gamma)K^+$; b), e), h) $D^{*0}(D^0\pi^0)K^+$ and c), f), i) $D^{*+}(D^0\pi^+)K^0_S$. The points with error bars are the data, while the curves show the fit result.

In summary, we report a measurement of the branching fractions for the decays $B \to D_{s1}(2536)^+\bar{D}^{(*)}$, where $\bar{D}^{(*)}$ is $\bar{D}^0$, D^- or D^{*-}. From a simultaneous fit to all B and $D_{s1}(2536)^+$ decay channels we measure $\mathcal{B}(B^+ \to D_{s1}(2536)^+\bar{D}^0) \times \mathcal{B}(D_{s1}(2536)^+ \to (D^{*0}K^+ + D^{*+}K^0)) = (3.97 \pm 0.85 \pm 0.56) \times 10^{-4}$, $\mathcal{B}(B^0 \to D_{s1}(2536)^+D^-) \times \mathcal{B}(D_{s1}(2536)^+ \to (D^{*0}K^+ + D^{*+}K^0)) = (2.75 \pm 0.62 \pm 0.36) \times 10^{-4}$ and $\mathcal{B}(B^0 \to D_{s1}(2536)^+D^{*-}) \times \mathcal{B}(D_{s1}(2536)^+ \to (D^{*0}K^+ + D^{*+}K^0)) = (5.01 \pm 1.21 \pm 0.70) \times 10^{-4}$. The ratio $\mathcal{B}(D_{s1} \to D^{*0}K^+)/\mathcal{B}(D_{s1} \to D^{*+}K^0)$ is measured to be $0.88 \pm 0.24 \pm 0.08$. The first error is statistical and the second one is systematic. The obtained results are consistent within errors with the previous measurements [7].

Using the latest measurements of the $B \to D^{(*)}D^{(*)}_{s(J)}$ branching fractions [1] we calculate the ratios discussed in [5]:

$$R_{D0} = \frac{\mathcal{B}(B \to DD^*_{s0}(2317))}{\mathcal{B}(B \to DD_s)} = 0.10 \pm 0.03,$$

$$R_{D^*0} = \frac{\mathcal{B}(B \to D^*D^*_{s0}(2317))}{\mathcal{B}(B \to D^*D_s)} = 0.15 \pm 0.06,$$

$$R_{D1} = \frac{\mathcal{B}(B \to DD_{s1}(2460))}{\mathcal{B}(B \to DD^*_s)} = 0.44 \pm 0.11,$$

$$R_{D^*1} = \frac{\mathcal{B}(B \to D^*D_{s1}(2460))}{\mathcal{B}(B \to D^*D^*_s)} = 0.58 \pm 0.12.$$

In addition, the same ratios are calculated for $B \to D^{(*)}D_{s1}(2536)^+$ decays using combined BaBar [7] and current results:

$$R_{D1'} = \frac{\mathcal{B}(B \to DD_{s1}(2536))}{\mathcal{B}(B \to DD^*_s)} = 0.049 \pm 0.010,$$

$$R_{D^*1'} = \frac{\mathcal{B}(B \to D^*D_{s1}(2536))}{\mathcal{B}(B \to D^*D^*_s)} = 0.044 \pm 0.010.$$

In these calculations it is assumed that the decay modes $D^*_{s0}(2317)^+ \to D^+_s\pi^0$ and $D_{s1}(2536)^+ \to (D^{*0}K^+ + D^{*+}K^0)$ are dominant.

According to [4, 5], within the factorization model and in the heavy quark limit, these ratios should be of order unity for the $D^*_{s0}(2317)$ and $D_{s1}(2460)$, whereas for the $D_{s1}(2536)$ they can be very small. From the above ratios we can conclude that while the decay pattern of the $D_{s1}(2536)$ follows the expectations, the new D_{sJ} states are either not canonical $c\bar{s}$ mesons, or this approach does not work for these particles.

We are grateful to A. Datta for useful discussions. We thank the KEKB group for the excellent operation of the accelerator, the KEK cryogenics group for the efficient operation of the solenoid, and the KEK computer group and the National Institute of Informatics for valuable computing and SINET3 network support. We acknowledge support from the Ministry of Education, Culture, Sports, Science, and Technology (MEXT)

of Japan, the Japan Society for the Promotion of Science (JSPS), and the Tau-Lepton Physics Research Center of Nagoya University; the Australian Research Council and the Australian Department of Industry, Innovation, Science and Research; the National Natural Science Foundation of China under contract No. 10575109, 10775142, 10875115 and 10825524; the Ministry of Education, Youth and Sports of the Czech Republic under contract No. LA10033 and MSM0021620859; the Department of Science and Technology of India; the BK21 and WCU program of the Ministry Education Science and Technology, National Research Foundation of Korea, and NSDC of the Korea Institute of Science and Technology Information; the Polish Ministry of Science and Higher Education; the Ministry of Education and Science of the Russian Federation and the Russian Federal Agency for Atomic Energy; the Slovenian Research Agency; the Swiss National Science Foundation; the National Science Council and the Ministry of Education of Taiwan; and the U.S. Department of Energy. This work is supported by a Grant-in-Aid from MEXT for Science Research in a Priority Area ("New Development of Flavor Physics"), and from JSPS for Creative Scientific Research ("Evolution of Tau-lepton Physics").

[1] K. Nakamura *et al.* (Particle Data Group), J. Phys. G **37**, 075021 (2010).
[2] H. Albrecht *et al.* (ARGUS Collaboration), Phys. Lett. B **230**, 162 (1989).
[3] The inclusion of charge-conjugate modes is implied throughout this Letter.
[4] A. Le Yaouanc, L. Oliver, O. Pene, J.-C. Raynal, Phys. Lett. B **387**, 582 (1996).
[5] A. Datta and P. O'Donnell, Phys. Lett. B **572**, 164 (2003).
[6] B. Aubert *et al.* (BaBar Collaboration), Phys. Rev. D **74**, 091101 (2006).
[7] B. Aubert *et al.* (BaBar Collaboration), Phys. Rev. D **77**, 011102 (2008).
[8] J. Dalseno *et al.* (Belle Collaboration), Phys. Rev. D **76**, 072004 (2007).
[9] A. Abashian *et al.* (Belle Collaboration), Nucl. Instr. and Meth. A **479**, 117 (2002).
[10] KEKB B Factory Design Report, KEK Report 95-1, 1995, unpublished.
[11] G.C. Fox and S. Wolfram, Phys. Rev. Lett. **41**, 1581 (1978).
[12] H. Albrecht *et al.* (ARGUS Collaboration), Phys. Lett. B **229**, 304 (1989).